Chapter 3

Successive Linearization of Heat and Mass Transfer over an Unsteady Stretching Permeable Surface in the Presence of Thermal Radiation and a Variable Chemical Reaction

Stanford Shateyi and Sandile S. Motsa

Additional information is available at the end of the chapter

http://dx.doi.org/10.5772/51228

1. Introduction

Theoretical studies of viscous incompressible flows over continuous stretching surfaces through a quiescent fluid have their origins in the pioneering work of Crane 1970. These types of flows occur in many industrial processes, such as in glass fibre production, food stuff processing reactor fluidization, and transpiration cooling. The prime aim in almost every extrusion is to maintain the surface quality of the extrudate. The pioneering works of Crane have been extended by many researchers to explore various aspects of the flow and heat and mass transfer occurring in infinite domains of the fluid surrounding the stretching sheet, [Liu and Andersson 2008; Abd EL-Aziz 2009; Abel and Mahesha 2008; Shateyi and Motsa 2009; Ziabakhsh et al. 2010; Motsa and Sibanda 2011], among others.

Many practical diffusive processes involve molecular diffusion of species in the presence of chemical reaction within and/or at the boundary. Chemical reaction can tremendously alter diffusion rates in convective heat and mass transfer processes. The effect of a chemical reaction depends on whether the reaction is heterogenous or homogeneous, as well as whether it occurs at an interface or a single phase volume reaction. We call a reaction of order n, if the reaction rate is proportional to the nth power of the concentration. The study of chemical reaction processes is useful for improving a number of chemical technologies such as polymer production and food processing. Various aspects of this problem have been studied by some researchers (Alam et al. 2009; Shateyi et al. 2010; Cortel 2007; Alam and Ahammad 2011; Afify and Elgazery 2012).

There has been much interest in the study of radiative heat transfer flows due to the effect of radiation on performance of many engineering systems applying electrically conducting fluids. Many engineering processes such as nuclear plants, gas turbines, satellites and space vehicles, take place at high temperatures and thus the effect of thermal radiation cannot be

ignored. Recently, flow, heat and/or mass transfer with thermal radiation have been studied by (Abd El-Aziz 2008; Shateyi and Motsa 2009; Pal and Mondal 2011).

In this chapter, we explore the semi analytic solution of the non linear heat and mass transfer over an unsteady stretching permeable surface with prescribed wall conditions in the presence of thermal radiation and a non-uniform chemical reaction. The proposed method of solution employed in this work is based on an extension of the quasilinearization method (QLM) that was initially proposed in Bellman and Kalaba (1965). This method employs Taylor series linearization to convert a nonlinear two-point boundary value problem into an iterative scheme of solution which can be integrated using various numerical techniques. Mandelzweig and his co-workers (see for example, Krivec et al. 1991; Mandelzweig 2005; Krivec and Mandelzweig 2008, among others) have recently extended the application of the QLM to a wide variety of nonlinear BVPs and established that the method converges quadratically. The integration of the QLM iteration scheme is performed using the Chebyshev spectral collocation method Canuto et al. 1988. Several studies (see for example, Awad et al.2011; Makukula et al. 2010a; Makukula et al. 2010b; Makukula et al. 2010c; Makukula et al. 2010d; Motsa 2011; Motsa and Shateyi 2010; Motsa 2011 and Shateyi Motsa 2011) have shown that blending the Chebyshev spectral method with iteration schemes like the QLM results in a highly accurate method which can be used to solve a wide variety of nonlinear boundary value problems.

In this work we present new iteration schemes which are based on systematically extending the QLM. The objective of this work is to demonstrate that the convergence rate of the QLM can be significantly improved by using the proposed iterations schemes.

2. Mathematical formulation

The study investigates the unsteady laminar boundary layer in a quiescent viscous incompressible fluid on a horizontal sheet which comes through a slot at the origin. At $t = 0$, the sheet is stretched with velocity $U_w(x,t)$ along the x-axis, keeping the origin in the fluid of ambient temperature T_∞ and concentration C_∞. The RosseLand approximation is used to describe the radiative heat flux in the energy equation. We also assume a variable chemical reaction.

The velocity, temperature and concentration fields in the boundary layer are governed by the two dimensional boundary layer equations for mass, and chemical species given by

$$\frac{\partial u}{\partial x} + \frac{\partial v}{\partial y} = 0, \tag{1}$$

$$\frac{\partial u}{\partial t} + u\frac{\partial u}{\partial x} + v\frac{\partial u}{\partial y} = \nu\frac{\partial^2 u}{\partial y^2}, \tag{2}$$

$$\frac{\partial T}{\partial t} + u\frac{\partial T}{\partial x} + v\frac{\partial T}{\partial y} = \alpha_0\frac{\partial^2 T}{\partial y^2} - \frac{1}{\rho cp}\frac{\partial q_r}{\partial y}, \tag{3}$$

$$\frac{\partial C}{\partial t} + u\frac{\partial C}{\partial x} + v\frac{\partial C}{\partial y} = D_m\frac{\partial^2 C}{\partial y^2} - K_l(C - C_\infty)^n, \tag{4}$$

Where u, v are the velocity components in the x and y directions,respectively, ν is the kinematic viscosity,g is the acceleration due to gravity, ρ is the density of the fluid, T and T_∞

http://dx.doi.org/10.5772/51228

are the temperature of the fluid inside the thermal boundary layer and of the fluid in the free stream, respectively while C and C_∞ are the corresponding concentrations, α_0 is the thermal diffusivity, c_p is the specific heat at constant pressure, D_m is the mass diffusivity and q_r is the radiative heat flux.

The boundary conditions are given as follows:

$$u = U_w, \ \ v = V_w, \ \ T = T_w, \ \ C = C_w \ \ \text{at} \ \ y = 0, \tag{5}$$

$$u \to 0, \ \ T \to T_\infty, \ \ C = C_\infty, \ \ \text{as} \ \ y \to \infty. \tag{6}$$

The stretching velocity $U_w(x,t)$, the surface temperature $T_w(x,t)$ and the surface concentration are assumed to be of the form: $U_w(x,t) = a/(1-ct)$, $T_w(x,t) = T_\infty + bx/(1-ct)$, $C_w(x,t) = C_\infty + bx/(1-ct)$, where a, b and c are positive constants with (ct<1), and both a and c have dimension reciprocal time.

The radiative heat flux q_r is described by the Rosseland approximation such that

$$q_r = -\frac{4\sigma^*}{3K}\frac{\partial T^4}{\partial y}, \tag{7}$$

where σ^* and K are the Stefan-Boltzman constant and the mean absorption coefficient, respectively. Following Chamkha (1997), we assume that the temperature differences within the flow are sufficiently small so that the T^4 can be expressed as a linear function after using Taylor series to expand T^4 about the free stream temperature T_∞ and neglecting higher order terms. This results in the following approximation

$$T^4 \approx 4T_\infty^3 T - 3T_\infty^4 \tag{8}$$

Using equations (7) and (8) in equation (3) we obtain

$$\frac{\partial q_r}{\partial y} = -\frac{16\sigma^* T_\infty^3}{3K}\frac{\partial^2 T}{\partial y^2}.$$

2.1. Similarity solutions

Now we introduce the following dimensionless functions of f, θ and ϕ and similarity variable η (Ishak et al., 2009).

$$\eta = \left(\frac{U_w}{\nu x}\right)^{\frac{1}{2}} y, \ \ \psi = (\nu x U_w)^{\frac{1}{2}} f(n), \ \ \theta(n) = \frac{T - T_\infty}{T_w - T_\infty}, \ \ \phi = \frac{C - C_\infty}{C_w - C_\infty}, \tag{9}$$

where

$\psi(x,y,t)$ is a stream function defined as $u = \frac{\partial \psi}{\partial y}$ and $v = -\frac{\partial \psi}{\partial x}$

The governing equations are then transformed into a set of ordinary equations and associated boundary conditions as given below:

$$f''' + ff'' - (f')^2 - A(f' + \frac{\eta}{2}f'') = 0, \tag{10}$$

$$(3R+4)\theta'' + 3RPr[f\theta' - 2f'\theta - \frac{A}{2}(3\theta + \eta\theta')] = 0, \tag{11}$$

$$\phi'' + Sc[f\phi' - 2f'\phi - \frac{A}{2}(3\phi + \eta\phi')] - ScK\phi^n = 0, \tag{12}$$

where A=c/a is the component that measures the unsteadiness, $Pr = \nu/\alpha$ is the Prandtl number, $R = 16\sigma T_\infty^3/3Kk$ is the radiation parameter, $Sc = \nu/D_m$ is the Schmidt number and $K = K_l(C_w - C_\infty)^{n-1}x/U_w(x,t)$ is the local chemical reaction parameter.

The boundary conditions are:

$$f(0) = f_w,\ f'(0) = 1,\ \phi(0) = 1,\ \theta(0) = 1, \tag{13}$$

$$f'(\infty) = 0,\ \theta(\infty) = 0,\ \phi(\infty) = 0, \tag{14}$$

with $f_w < 0$ and $f_w > 0$ corresponding to injection and suction, respectively.

3. Method of solution

To solve the governing system of equations (12 - 14) we observe that equation (10) depends on $f(\eta)$ only. Thus, it can be solved independently of the other equations in the system. The solution for $f(\eta)$ is then substituted in equations (11) and (12) which can also be solved for θ and ϕ separately. We begin by obtaining the solution for $f(\eta)$. We assume that an estimate of the the solution of (10) is f_γ. For convenience, we introduce the following notation

$$f_0 = f, \quad f_1 = f', \quad f_2 = f'', \quad f_3 = f'''. \tag{15}$$

In terms of the new variables (15), equation (10) can be written as

$$L[f_0, f_1, f_2, f_3] + N[f_0, f_1, f_2, f_3] = 0, \tag{16}$$

where

$$L[f_0, f_1, f_2, f_3] = f_3 - A(f_1 + \frac{\eta}{2}f_2), \quad N[f_0, f_1, f_2, f_3] = f_0 f_2 - f_1^2 \tag{17}$$

We introduce the following coupled system,

$$L[f_0, \ldots, f_3] + N(f_{0,\gamma}, \ldots, f_{3,\gamma}) + \sum_{s=0}^{3}(f_s - f_{s,\gamma})\frac{\partial N}{\partial f_s}(f_{0,\gamma}, \ldots, f_{3,\gamma}) + G(f_0, \ldots, f_3) = 0, \tag{18}$$

$$G(f_0, \ldots, f_3) = N(f_0, \ldots, f_3) - N(f_{0,\gamma}, \ldots, f_{3,\gamma}) - \sum_{s=0}^{3}(f_s - f_{s,\gamma})\frac{\partial N}{\partial f_s}(f_{0,\gamma}, \ldots, f_{3,\gamma}). \tag{19}$$

http://dx.doi.org/10.5772/51228

Note that when equations (18) and (19) are added, we obtain equation (16). Separating the known and unknown variables, equation (18) can be written as

$$L[f_0,\ldots,f_3]+\sum_{s=0}^{3} f_s\frac{\partial N}{\partial f_s}(f_{0,\gamma},\ldots,f_{3,\gamma})+G(f_0,\ldots,f_3)=0 \tag{20}$$

where

$$H(f_{0,\gamma},\ldots,f_{3,\gamma})=\sum_{s=0}^{3} f_{s,\gamma}\frac{\partial N}{\partial f_s}(f_{0,\gamma},\ldots,f_{3,\gamma})-N(f_{0,\gamma},\ldots,f_{3,\gamma}) \tag{21}$$

We use the quasilinearization method (QLM) of Bellman and Kalaba (1965) to solve equation (20). The QLM determines the $(i+1)$th iterative approximation $f_{s,i+1}$ as the solution of the differential equation

$$\begin{aligned} &L[f_{0,i+1},\ldots,f_{3,i+1}]+\sum_{s=0}^{3} f_{s,i+1}\frac{\partial N}{\partial f_s}(f_{0,\gamma},\ldots,f_{3,\gamma})+G(f_{0,i},\ldots,f_{3,i}) \\ &+\sum_{s=0}^{3}(f_{s,i+1}-f_{s,i})\frac{\partial G}{\partial f_s}(f_{0,i},\ldots,f_{3,i})=H(f_{0,\gamma},\ldots,f_{3,\gamma}). \end{aligned} \tag{22}$$

Separating the unknowns $f_{s,i+1}$ from the known functions $f_{s,i}$ yields

$$\begin{aligned} L[f_{0,i+1},\ldots,f_{3,i+1}]+\sum_{s=0}^{3}\left[\frac{\partial N}{\partial f_s}(f_{0,\gamma},\ldots,f_{3,\gamma})+\frac{\partial G}{\partial f_s}(f_{0,i},\ldots,f_{3,i})\right]f_{s,i+1}= \\ \sum_{s=0}^{3} f_{s,i}\frac{\partial G}{\partial f_s}(f_{0,i},\ldots,f_{3,i})-G(f_{0,i},\ldots,f_{3,i})+H(f_{0,\gamma},\ldots,f_{3,\gamma}), \end{aligned} \tag{23}$$

subject to

$$f_{0,i+1}(0)=0,\quad f_{1,i+1}(0)=1,\quad f_{1,i+1}(\infty)=0, \tag{24}$$

We assume that $f_{s,0}$ is obtained as a solution of the linear part of equation (20) given by

$$L[f_{1,0},\ldots,f_{3,0}]+\sum_{s=0}^{3} f_{s,0}\frac{\partial N}{\partial f_s}(f_{0,\gamma},\ldots,f_{3,\gamma})=H(f_{0,\gamma},\ldots,f_{3,\gamma}), \tag{25}$$

which yields the iteration scheme

$$L[f_{0,r+1},\ldots,f_{3,r+1}]+\sum_{s=0}^{3} f_{s,r+1}\frac{\partial N}{\partial f_s}(f_{0,r},\ldots,f_{3,r})=H(f_{0,r},\ldots,f_{3,r}). \tag{26}$$

It can easily be shown that equation (26) is the standard QLM iteration scheme for solving (16).

When $i = 0$ in (23) we can approximate f_s as

$$f_s \approx f_{s,1}. \tag{27}$$

Thus, setting $i = 0$ in (23) we obtain

$$L[f_{0,1}, \ldots, f_{3,1}] + \sum_{s=0}^{3} \left[\frac{\partial N}{\partial f_s}(f_{0,\gamma}, \ldots, f_{3,\gamma}) + \frac{\partial G}{\partial f_s}(f_{0,0}, \ldots, f_{3,0}) \right] f_{s,1} =$$
$$\sum_{s=0}^{3} f_{s,0} \frac{\partial G}{\partial f_s}(f_{0,0}, \ldots, f_{3,0}) - G(f_{0,0}, \ldots, f_{3,0}) + H(f_{0,\gamma}, \ldots, f_{3,\gamma}), \tag{28}$$

which yields the iteration scheme

$$L[f_{0,r+1}, \ldots, f_{3,r+1}] + \sum_{s=0}^{3} \left[\frac{\partial N}{\partial f_s}(f_{0,r}, \ldots, f_{3,r}) + \frac{\partial G}{\partial f_s}(f^{(0)}_{0,r+1}, \ldots, f^{(0)}_{3,r+1}) \right] f_{s,r+1} =$$
$$\sum_{s=0}^{3} f^{(0)}_{s,r+1} \frac{\partial G}{\partial f_s}(f^{(0)}_{0,r+1}, \ldots, f^{(0)}_{3,r+1}) - G(f^{(0)}_{0,r+1}, \ldots, f^{(0)}_{3,r+1}) + H(f_{0,r}, \ldots, f_{3,r}) \tag{29}$$

where $f^{(0)}_{s,r+1}$ is the solution of

$$L[f^{(0)}_{0,r+1}, \ldots, f^{(0)}_{3,r+1}] + \sum_{s=0}^{3} f^{(0)}_{s,r+1} \frac{\partial N}{\partial f_s}(f_{0,r}, \ldots, f_{3,r}) = H(f_{0,r}, \ldots, f_{3,r}). \tag{30}$$

The general iteration scheme obtained by setting $i = m$ ($m \geq 2$) in equation (23), hereinafter referred to as scheme-m is

$$L[f_{0,r+1}, \ldots, f_{3,r+1}] + \sum_{s=0}^{3} \left[\frac{\partial N}{\partial f_s}(f_{0,r}, \ldots, f_{3,r}) + \frac{\partial G}{\partial f_s}(f^{(m-1)}_{0,r+1}, \ldots, f^{(m-1)}_{3,r+1}) \right] f_{s,r+1} =$$
$$\sum_{s=0}^{3} f^{(m-1)}_{s,r+1} \frac{\partial G}{\partial f_s}(f^{(m-1)}_{0,r+1}, \ldots, f^{(m-1)}_{3,r+1}) - G(f^{(m-1)}_{0,r+1}, \ldots, f^{(m-1)}_{3,r+1}) + H(f_{0,r}, \ldots, f_{3,r}) \tag{31}$$

http://dx.doi.org/10.5772/51228

where $f_{s,r+1}^{(m-1)}$ is obtained as the solution of

$$L[f_{0,r+1}^{(m-1)},\ldots,f_{3,r+1}^{(m-1)}]+\sum_{s=0}^{3}\left[\frac{\partial N}{\partial f_s}(f_{0,r},\ldots,f_{3,r})+\frac{\partial G}{\partial f_s}(f_{0,r+1}^{(m-2)},\ldots,f_{3,r+1}^{(m-2)})\right]f_{s,r+1}^{(m-1)}=$$

$$\sum_{s=0}^{3}f_{s,r+1}^{(m-2)}\frac{\partial G}{\partial f_s}(f_{0,r+1}^{(m-2)},\ldots,f_{3,r+1}^{(m-2)})-G(f_{0,r+1}^{(m-2)},\ldots,f_{3,r+1}^{(m-2)})+H(f_{0,r},\ldots,f_{3,r}) \tag{32}$$

The iterative schemes (26) and (31) can easily be solved using numerical methods such as finite differences, finite elements, Runge-Kutta based shooting methods or collocation methods. Several studies, (see for example, Awad et al.2011; Makukula et al. 2010a; Makukula et al. 2010b; Makukula et al. 2010c; Makukula et al. 2010d; Motsa 2011; Motsa and Shateyi 2010; Motsa 2011 and Shateyi Motsa 2011), have shown that the Chebyshev spectral collocation (CSC) method is very robust in solving iterations schemes of the type discussed in this work. The CSC method is based on approximating the unknown functions by the Chebyshev interpolating polynomials in such a way that they are collocated at the Gauss-Lobatto points defined as

$$z_j=\cos\frac{\pi j}{M},\qquad j=0,1,\ldots,M. \tag{33}$$

where M is the number of collocation points used (see for example Canuto et al. 1988, Trefethen 2000). For the convenience of numerical implementation, the domain $[0,\infty)$ is truncated as $[0,L_e]$ where L_e is chosen to be a sufficiently large real number. In order to implement the method, the physical region $[0,L_e]$ is transformed into the region $[-1,1]$ using the mapping

$$\eta=L_e\frac{z+1}{2},\quad -1\leq z\leq 1 \tag{34}$$

The derivatives of f at the collocation points are represented as

$$\frac{d^nf}{d\eta^n}=\sum_{k=0}^{M}\mathbf{D}_{kj}^2f(z_k),\quad j=0,1,\ldots,M \tag{35}$$

where $\mathbf{D}=2D/Le$, with D being the Chebyshev spectral differentiation matrix (see for example, Canuto et al. 1988, Trefethen 2000). Thus, applying the CSC on the functions f_s we obtain

$$f_s=\mathbf{D}^s\mathbf{F} \tag{36}$$

where $\mathbf{F}=[f_0(z_0),f_0(z_1),\ldots,f_0(z_{M-1}),f_0(z_M)]^T$.

Thus, applying the spectral method, with derivative matrices on equation (26) and the corresponding boundary conditions gives the following matrix system

$$\mathbf{C}_r\mathbf{F}_{r+1}=\mathbf{H}_r \tag{37}$$

with the boundary conditions

$$f_{0,r+1}(z_M) = 0, \quad \sum_{k=0}^{M} \mathbf{D}_{Mk} f_{0,r+1}(z_k) = 0, \quad \sum_{k=0}^{M} \mathbf{D}_{0k} f_{0,r+1}(z_k) = 1, \tag{38}$$

where

$$\mathbf{C}_r = \mathbf{D}^3 + \left(\mathbf{a}_{2,r} - \frac{A}{2}\eta_d\right)\mathbf{D}^2 + (\mathbf{a}_{1,r} - A)\mathbf{D} + \mathbf{a}_{0,r}. \tag{39}$$

The vector $\mathbf{H}_r$ corresponds to the function H when evaluated at the collocation points and $\mathbf{a}_{s,r}$ $(s = 0, 1, 2)$ is a diagonal matrix corresponding to the vector of $a_{i,r}$ which is defined as

$$a_{s,r} = \frac{\partial N}{\partial f_s} \tag{40}$$

and η_d is an $(M+1) \times (M+1)$ diagonal matrix of η. The boundary conditions (38) are imposed on the first, Mth and $(M+1)$th rows of C_r and $\mathbf{H}_r$ to obtain

$$\begin{pmatrix} \mathbf{D}_{0,0} & \mathbf{D}_{0,1} & \cdots & \mathbf{D}_{0,M-1} & \mathbf{D}_{0,M} \\ & & \mathbf{C_r} & & \\ \mathbf{D}_{M,0} & \mathbf{D}_{M,1} & \cdots & \mathbf{D}_{M,M-1} & \mathbf{D}_{M,M} \\ 0 & 0 & \cdots & 0 & 1 \end{pmatrix} \begin{pmatrix} f_{0,r+1}(z_0) \\ f_{0,r+1}(z_1) \\ \vdots \\ f_{0,r+1}(z_{M-2}) \\ f_{0,r+1}(z_{M-1}) \\ f_{0,r+1}(z_M) \end{pmatrix} = \begin{pmatrix} 1 \\ H_r(z_1) \\ \vdots \\ H_r(z_{N-2}) \\ 0 \\ 0 \end{pmatrix} \tag{41}$$

Starting from a suitable initial guess $f_{0,0}(\eta)$, the iteration scheme (41) can be used to iteratively give approximate solutions of the governing equation (10). The application of the CSC on the general iteration schemes (31) and (32) can be done in a similar manner for any value of m.

4. Results and discussion

In this section we present the results for the governing physical parameters of interest. In applying the Chebyshev spectral method described in the previous section $M = 100$ collocation points were used. The value of L_e for numerically approximating infinity was chosen to be $Le = 20$. In order to assess the accuracy of the proposed iteration methods, the present numerical results were compared against results generated using the MATLAB routine `bvp4c`. For illustration purposes, results are presented for the first three iterations schemes obtained by setting $m = 0, 1, 2$.

In Table 1 we give a comparison between the results of scheme-0 against results generated using `bvp4c`. We observe that the QLM results converge very rapidly to the `bvp4c` results. It takes only three or four iterations to achieve an exact match that is accurate to order 10^{-8} for the selected parameters of A. We also observe in this table that stretching increases the absolute values of the skin friction.

http://dx.doi.org/10.5772/51228

iter.	$A = 0$	$A = 0.5$	$A = 1$	$A = 1.5$	$A = 2$
1	-1.000000000	-1.166255146	-1.317872855	-1.455413216	-1.581765234
2	-1.000000000	-1.167211134	-1.320520326	-1.459662889	-1.587362322
3	-1.000000000	-1.167211513	-1.320522065	-1.459665895	-1.587366111
4	-1.000000000	-1.167211515	-1.320522065	-1.459665895	-1.587366111
5	-1.000000000	-1.167211517	-1.320522065	-1.459665895	-1.587366111
bvp4c	-1.000000000	-1.167211517	-1.320522065	-1.459665895	-1.587366111

Table 1. Comparison of the bvp4c values of $f''(0)$ at different values of A for Scheme-0 (QLM)

iter.	$A = 1$	$A = 2$	$A = 3$	$A = 4$
		Scheme-0		
1	-1.215913833273934	-1.508012270141307	-1.750647835613831	-1.963118416905635
2	-1.315711765474042	-1.586229425552791	-1.816415412229436	-2.022058898487201
3	-1.320495400678920	-1.587365641569519	-1.816850675892770	-2.020976536521761
4	-1.320522063086358	-1.587366111631070	-1.816849325533777	-2.020950025633773
5	-1.320522064602713	-1.587366111619306	-1.816849325468859	-2.020950025517386
6	-1.320522064602713	-1.587366111619306	-1.816849325468859	-2.020950025517386
		Scheme-1		
1	-1.315711765474042	-1.586229425552791	-1.816415412229436	-2.022058898487201
2	-1.320522063086358	-1.587366111631070	-1.816849325533777	-2.020950025633773
3	-1.320522064602713	-1.587366111619306	-1.816849325468859	-2.020950025517386
4	-1.320522064602713	-1.587366111619306	-1.816849325468859	-2.020950025517386
5	-1.320522064602713	-1.587366111619306	-1.816849325468859	-2.020950025517386
6	-1.320522064602713	-1.587366111619306	-1.816849325468859	-2.020950025517386
		Scheme-2		
1	-1.315240928788073	-1.585906261457893	-1.816236653612290	-2.021499891062478
2	-1.320522059975388	-1.587366111619187	-1.816849325470411	-2.020950025519239
3	-1.320522064602713	-1.587366111619306	-1.816849325468859	-2.020950025517386
4	-1.320522064602713	-1.587366111619306	-1.816849325468859	-2.020950025517386
5	-1.320522064602713	-1.587366111619306	-1.816849325468859	-2.020950025517386
6	-1.320522064602713	-1.587366111619306	-1.816849325468859	-2.020950025517386

Table 2. $f''(0)$ at different values of A for scheme-0,1,2

iter.	$A = 1$	$A = 2$	$A = 3$	$A = 4$
		Scheme-0		
1	0.104608231328780	0.079353841477999	0.066201489855027	0.057831608611751
2	0.004810299128671	0.001136686066515	0.000433913239423	0.001108872969816
3	0.000026663923793	0.000000470049787	0.000001350423911	0.000026511004376
4	0.000000001516355	0.000000000011764	0.000000000064918	0.000000000116388
5	0.000000000000000	0.000000000000000	0.000000000000000	0.000000000000000
6	0.000000000000000	0.000000000000000	0.000000000000000	0.000000000000000
		Scheme-1		
1	0.004810299128671	0.001136686066515	0.000433913239423	0.001108872969816
2	0.000000001516355	0.000000000011764	0.000000000064918	0.000000000116388
3	0.000000000000000	0.000000000000000	0.000000000000000	0.000000000000000
4	0.000000000000000	0.000000000000000	0.000000000000000	0.000000000000000
5	0.000000000000000	0.000000000000000	0.000000000000000	0.000000000000000
6	0.000000000000000	0.000000000000000	0.000000000000000	0.000000000000000
		Scheme-2		
1	0.005281135814640	0.001459850161413	0.000612671856568	0.000549865545092
2	0.000000004627325	0.000000000000119	0.000000000001552	0.000000000001853
3	0.000000000000000	0.000000000000000	0.000000000000000	0.000000000000000
4	0.000000000000000	0.000000000000000	0.000000000000000	0.000000000000000
5	0.000000000000000	0.000000000000000	0.000000000000000	0.000000000000000
6	0.000000000000000	0.000000000000000	0.000000000000000	0.000000000000000

Table 3. $f''(0)$ at different values of A

Tables 2 and 3 give the results of the comparison of the values of $f''(0)$ between three levels of the iteration schemes and their corresponding errors. In computing the errors it was assumed that the result corresponding to the 6th iteration is the converged solution. From numerical experimentation it was found that all the iteration schemes would have completely converged to a fixed value by the time the 5th or 6th iteration is used. The results from Table 2 and 3 clearly indicate that the the convergence to the solution progressively improves when you use the higher level iteration schemes. For instance, from Table 3 we note that it takes only 2 iterations to achieve full convergence in scheme-1 and scheme-2 compare to four iterations in scheme-0. This results demonstrates the improvement offered by the proposed new iteration scheme on the original quasilinearization method which corresponds to scheme-0.

In Figs. 1 - 7 we give illustrations showing the effect of the governing parameters on the flow properties. Unless otherwise specified, the sample illustrations were generated using $R = 1$, $Pr = 0.7$, $Sc = 1$, $K = 1$, $A = 1$. In Figs. 1 - 3 we show the velocity, temperature and concentration profiles for different values of A. In Fig. 1 we observe that the velocity $f'(\eta)$ is a monotonically decreasing function of the stretching parameter A. From Figs. 2 and 3, we observe that both the temperature and concentration distributions are reduced as values of the stretching parameter increase. The velocity, thermal and solutal boundary layer thicknesses all decrease as the values of A increase. As a consequence the transition from

http://dx.doi.org/10.5772/51228

laminar flow to turbulent flow is delayed. This shows that stretching of surfaces can be used as a flow stabilizing mechanism.

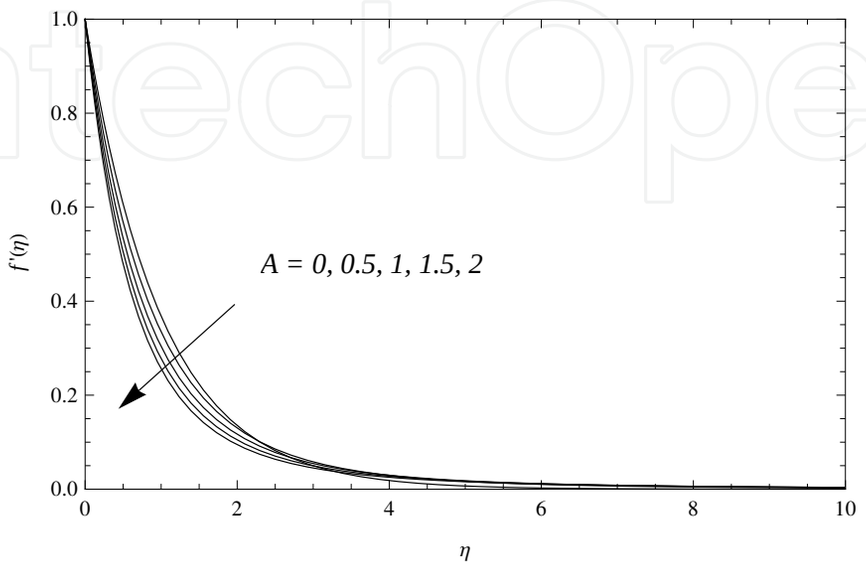

Figure 1. The variation of A on the flow velocity, $f'(\eta)$

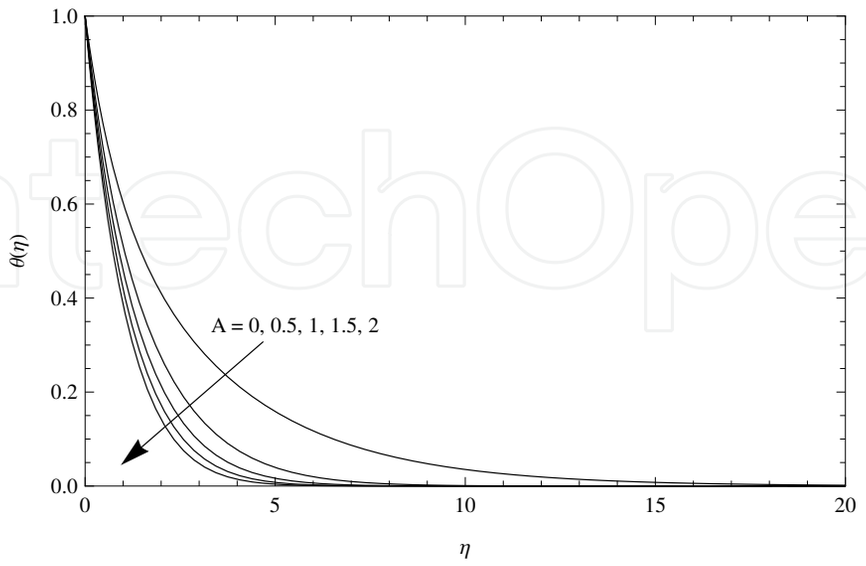

Figure 2. Effect of A on the fluid temperature, $\theta(\eta)$

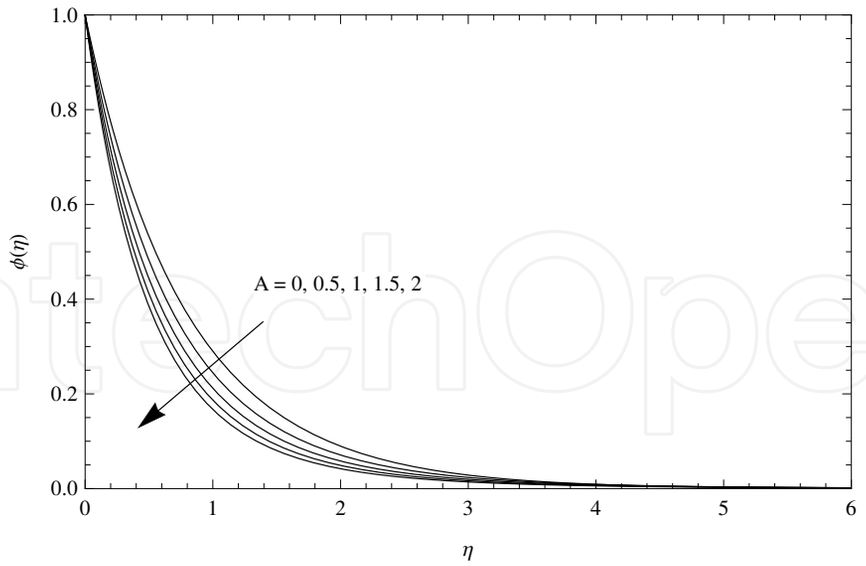

Figure 3. Effect of A on the fluid concentration, $\phi(\eta)$

Fig. 4 depicts the effects of the Prandtl number on the temperature distributions. We observe that as Pr increases, the temperature profiles and the thermal boundary layer thickness become smaller. This is because when Pr increases, the thermal diffusivity decreases, leading to the decrease of the energy transfer ability that decreases the thermal boundary layer. The effect of thermal radiation R on the temperature field is shown in Fig. 5. From this figure we see that the effect of increasing the thermal radiation parameter R is to reduce the temperature profiles.

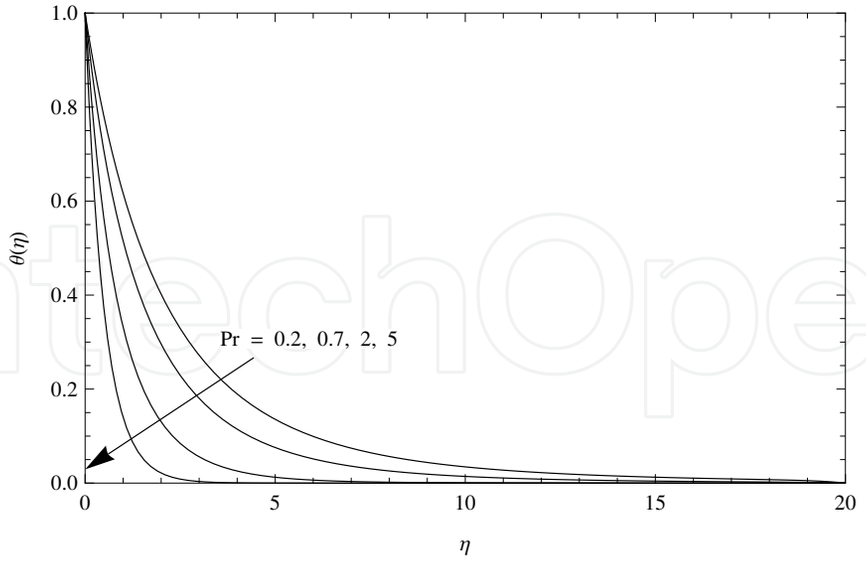

Figure 4. Temperature profiles for various values of Pr

Fig. 6 shows the dimensionless concentration profiles for different values of the Schmidt number Sc. We clearly see from this figure that the concentration boundary layer thickness

http://dx.doi.org/10.5772/51228

decreases as the Schmidt number Sc increases. This phenomenon occurs because when Sc, the mass diffusivity decreases and the fluid becomes heavier. The effects of chemical reaction K on the concentration distributions is displayed in Fig. 7. It should be noted here that physically positive values of K implies the destructive reaction. We observe in this figure that an increase in the chemical reaction leads to the decrease in the concentration can profiles. This shows that diffusion rate can be tremendously altered by chemical reaction.

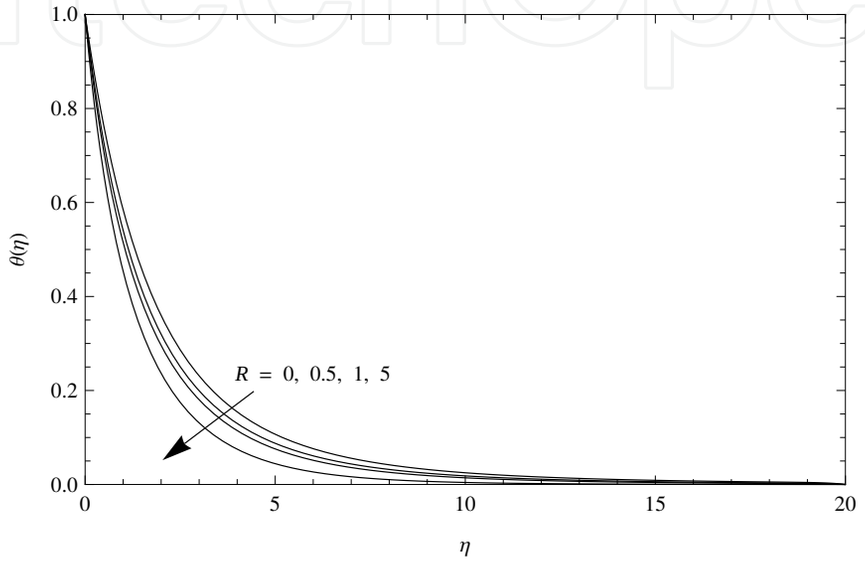

Figure 5. Effect of R on the fluid temperature, $\theta(\eta)$

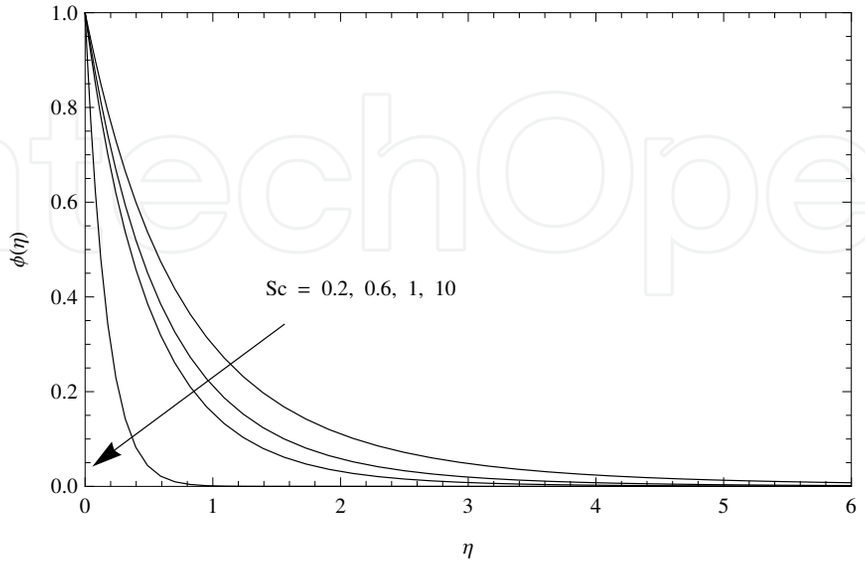

Figure 6. Effect of Sc on the solute concentration, $\phi(\eta)$

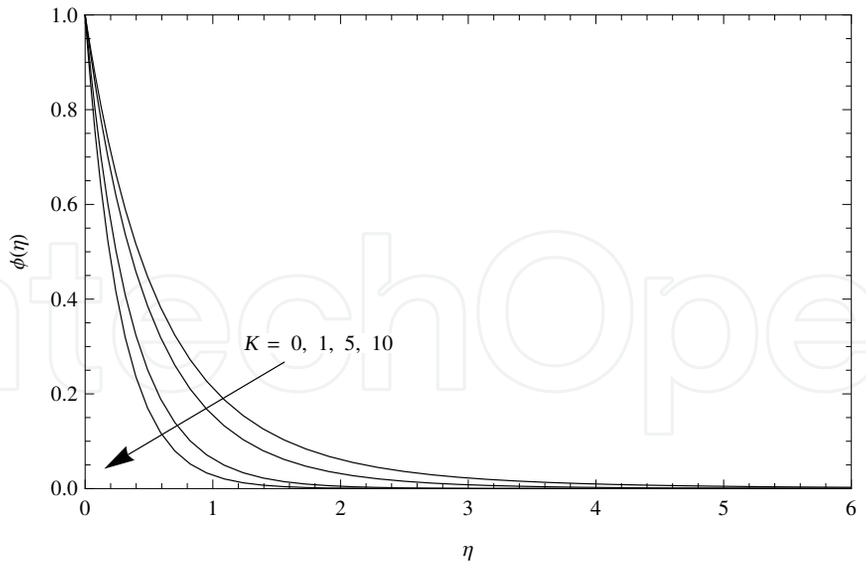

Figure 7. The solute concentration profiles for various values of K.

5. Conclusion

In this chapter we explored the semi-analytic solution of the non linear heat and mass transfer flow over an unsteady stretching permeable surface with prescribed wall conditions in the presence of thermal radiation and non-uniform chemical reaction. From the present investigation we may conclude the following:

1. Blending the QLM scheme with Chebyshev spectral collocation method leads to more accurate and faster convergence scheme.
2. Radiation significantly affect the fluid flow properties.
3. The diffusion rate is significantly altered by chemical radiation.
4. The velocity, temperature and concentration profiles decrease with increasing values of the stretching parameter A.

Author details

Stanford Shateyi[1] and Sandile S. Motsa[2]

[1]University of Venda, South Africa
[2]University of KwaZulu-Natal, South Africa

6. References

[1] Abd El-Aziz, M. (2008). Thermal-diffusion and diffusion-thermo effects on combined heat and mass transfer by hydromagnetic three-dimensional free convection over a permeable stretching surface with radiation. *Physics Letters A*. 372, 263-372.

[2] Abd El-Aziz, M. (2009). Radiation effect on the flow and heat transfer over an unsteady stretching sheet, *Int. Commun. Heat Mass Transf*, doi:10.1016/j.icheatmasstransfer.2009.01.016.

[3] Abel, M.S. & Mahesha, N. (2009). Heat transfer in MHD viscoelastic fluid over a stretching sheet with variable thermal conductivity, non-uniform heat source and radiation. *Appl. Math. Modell.* 32, 1965-1983.

[4] Alam, M.S., Rahman, M.M., & Sattar, M.A. (2009). Transient Magnetohydrodynamic Free Convective Heat and Mass Transfer Flow with Thermophoresis past a Radiative Inclined Permeable Plate in the Presence of Variable Chemical Reaction and Temperature Dependent Viscosity. *Nonlinear Analysis: Modelling and Control.* 14., 1., pp 3-20.

[5] Alam, M.S., & Ahammad, M.U.(2011). Effects of variable chemical reaction and variable electric conductivity on free convective heat and mass transfer flow along an inclined stretching sheet with variable heat and mass fluxes under the influence of Dufour and Soret effects. *Nonlinear Analysis: Modelling and Control*. 16.1., pp 1-16.

[6] Afify, A.A., & Elgazery, N.S. (2012). Lie group analysis for the effects of chemical reaction on MHD stagnation-point flow of heat and mass transfer towards a heated porous stretching sheet with suction or injection. *Nonlinear Analysis: Modelling and Control*. 17.1. pp 1-15.

[7] Awad, F.G. Sibanda, P. Motsa, S.S. & Makinde, O.D. (2011). Convection from an inverted cone in a porous medium with cross-diffusion effects, *Computers and Mathematics with Applications,* 61, pp 1431–1441.

[8] Bellman. R.E., & R.E. Kalaba, (1965), Quasilinearization and Nonlinear Boundary-Value Problems, *Elsevier, New York.*

[9] Canuto, C, Hussaini, M.L, Quarteroni, A. & Zang, T.A. (1988). Spectral Methods in Fluid Dynamics. *Springer-Verlag, Berlin.*

[10] Chamkha, A. J., (1997). Hydromagnetic natural convetion from an isothermal inclined surface adjacent to a thermally stratified porous medium, *Int. J. Eng. Sci.*, 37, 10.11, pp 975 - 986.

[11] Crane, L. J. (1970). Flow past a stretching plate, *Z. Angew. Math. Physc.* 12, pp 645-647.

[12] Cortell, R. (2007). MHD flow and mass transfer of an electrically conducting fluid of second grade in a porous medium over a stretching sheet with chemically reactive species. *Chemical Engineering and Processing*. 46, pp 721-728.

[13] Ishak, A., Nazar, R., and Pop, I. (2009). Heat Transfer over an Unsteady Stretching Permeable Surface with Prescribed Temperature, *Nonlinear Analysis: Real World Applications*, 10, pp 2909-2913.

[14] Krivec, R.; Haftel, M.I. & Mandelzweig, V.B. (1991). Precisse nonvariational calculation of excited states of helium with the correction-function hyperspherical-harmonic method. *Physical Review A.* Vol. 44. No. 11. pp 7159-7164. December 1991.

[15] Krivec, R. & Mandelzweig, V.B. (2008). Quasilinearization approach to computations to computations with singular potentials. *Computer Physics Communications.* Vol. 179. pp 865-867.

[16] Chung Liu I & Andersson, H.L. (2008).Heat transfer in a liquid film on an unsteady stretching sheet, *International Journal of Thermal Sciences,* 47, pp 766-772.

[17] Makukula, Z.G. Sibanda, P.& Motsa, S.S. (2010a). A novel numerical technique for two-dimensional laminar flow between two moving porous walls, *Mathematical Problems in Engineering* Article ID 528956, pp 1-15; doi:10.1155/2010/528956.

[18] Makukula, Z.G. Sibanda, P.& Motsa, S.S. (2010b) A note on the solution of the von KÃąrmÃąn equations using series and Chebyshev spectral methods. *Boundary Value Problems,* Vol. 2010, Article ID 471793, pp 1-17 ; doi:10.1155/2010/471793.

[19] Makukula, Z.G., Sibanda, P., & Motsa, (2010c). On new solutions for heat transfer in a visco-elastic fluid between parallel plates. *International Journal of Mathematical Models and Methods in Applied Sciences*. 4, (4), pp 221 - 230.

[20] Makukula, Z.G., Motsa, S.S., & P. Sibanda. (2010). On a new solution for the viscoelastic squeezing flow between two parallel plates, *Journal of Advanced Research in Applied Mathematics.* 2, pp 31 - 38.

[21] Mandelzweig, V.B. (2005). Quasilinearization Method: Nonperturbative Approach to Physical Problems. *Physics of Atomic Nuclei.* Vol. 68. No. 7. pp 1228-1257.

[22] Motsa, S.S.& Shateyi,S. (2010). A New Approach for the Solution of Three-Dimensional Magnetohydrodynamic Rotating Flow over a Shrinking Sheet, *Mathematical Problems in Engineering,* vol. 2010, Article ID 586340, pp 1-15. doi:10.1155/2010/586340

[23] Motsa, S.S., & Sibanda, P., (2011). On the solution of MHD flow over a nonlinear stretching sheet by an efficient semi-analytical technique, *Int.J Numer.fluids*, pp 1-13.

[24] Motsa, S.S. (2011). New algorithm for solving non-linear BVPs in heat transfer, *International Journal of Modeling, Simulation & Scientific Computing*, 2(3), pp 355–373.

[25] Motsa, S.S. & Shateyi,S. (2011). Successive Linearisation Solution of Free Convection Non-Darcy Flow with Heat and Mass Transfer, *Advanced Topics in Mass Transfer*, Mohamed El-Amin (Ed.), pp 425-438, InTech Open Access Publishers.

[26] Pal, D., & Mondal, H., (2011). Hydromagnetic non-Darcy flow and heat transfer iver a stretching sheet in the presence of thermal radiation and Ohmic dissipation. *Commun Nonlinear Sci Numer Simulat*. 15. 1197-1209.

[27] Shateyi, S. Motsa, S.S., (2009). Thermal radiation effects on heat and mass transfer over an unsteady stretching surface, *Mathematical Problems in Engineering*, Vol. 2009, doi:10.1155/2009/965603.

[28] Shateyi, S., Motsa, S.S., & Sibanda, P. (2010). Homotopy analysis of heat and mass transfer boundary layer flow through a non-porous channel with chemical reaction and heat generation. *The Canadian Journal of Chemical Engineering*. 88. pp 975-982.

[29] Shateyi, S., Motsa, S.S., (2010). Variable viscosity on magnetohydrodynamic fluid flow and heat transfer over an unsteady stretching surface with Hall effect, *Boundary Value Problems*, Vol. 2010, Article ID 257568, pp 1-20, doi:10.1155/2010/257568

[30] Trefethen, L.N., Spectral Methods in MATLAB, SIAM, 2000

[31] Zibakhsh, Z., Domairry, G., Mozaffari, M., & Mahbobifar, M. (2010). Analytical solution of heat transfer over an unsteady stretching permeable surface with prescribed wall temperature. *Journal of the Taiwan Institute of Chemical Engineers*. 41, pp 169-177.

IntechOpen